Additive Manufacturing 36 (2020) 101440

Contents lists available at ScienceDirect

Additive Manufacturing

journal homepage: www.elsevier.com/locate/addma

Inverted multi-material laser sintering

John Whitehead*, Hod Lipson

Department of Mechanical Engineering, 500 W 120th Street, Mudd #220, Columbia University, New York, NY, USA

ARTICLE INFO

Keywords:
Additive manufacturing
Selective laser sintering
Inverted printing
Multi-material
Powder bed fusion

ABSTRACT

We present an additive manufacturing process that uses an upward-directed laser to fuse a monolayer of powder onto a substrate through a clear surface. The process is then repeated to build a hanging part layer by layer, by replenishing powder on the glass, or moving to a second plate with a different powder. Our process eliminates the need for a large powder bed as well as allows the sintering of different powders in a single layer. We demonstrate this method by using a 445 nm laser to fabricate a multi-material pattern of Nylon-12 and TPU. We characterize the mechanical properties of the fabricated composite and discuss advantages and disadvantages of this approach.

1. Introduction

1.1. Selective laser sintering

The field of additive manufacturing (AM) has experienced persistent growth over the past decade, with an annual rate surpassing 20% [1]. Laser Sintering (LS) is the most widely used AM method of the industrial processes and is responsible for the largest portion of that growth [2,3]. Traditionally, LS works by using downward-directed lasers to sinter together microscale material particles within a powder bed, in order to generate a finished part. Parts are built up from particles layer by layer, with the unsintered particles acting as support material for any thin or overhanging sections of the printing part.

The LS process can accomodate a wide range of materials, including a variety of thermoplastics and metals [4–7], and generates highly durable parts with strengths typically superior to parts generated through other AM processes. LS can also manufacture a variety of geometries with high complexities, such as lattices, which are challenging to fabricate using other AM processes. Furthermore, in contrast to most other AM processes, parts generated on an LS machine can be used as functional end use pieces [8]. These benefits have enabled LS processes to revolutionize a variety of fields, including industries such as defense, biomedical and aerospace [9,10].

Despite their industry-wide adoption, traditional LS processes have several major disadvantages. First, LS processes require a full powder bed that is frequently heated to near-melt temperatures in order to facilitate particle sintering [11]. This ambient heating can cause chemical and physical changes which negatively affect material predictability, resulting in the unfused particles being thrown out or requiring a transfusion of unheated material to be useable [12,13].

Second, the unfused powder bed, while sometimes necessary to support a part, has the downside of making the printed part challenging to monitor in full. While some advanced LS systems use optical feedback [14,15], they can monitor only the exposed top surface of the printed part, and will not detect warping occurring in covered lower layers. This can further contribute to the waste generated by traditional LS processes, as any parts which have failed to print properly will be discarded and re-printed, wasting both the material used in the failed print, and the powder affected by the new print.

An additional key disadvantage of LS processes is they usually only allow for sintering a single material at a time [16–18].

1.2. Multi-material printing

Due to the large variety of available materials, a successful multi-material AM process would have a wide array of practical applications, such as the development of graded alloys, or the ability to fabricate parts out of multiple types of thermoplastic polymers such as rigid components with overmolds.

Previous work has focused on developing multi-material AM methods for laser sintering equipment, either by replacing un-sintered material in a given layer with a secondary powder using a vacuum, or by placing an initial layer with spaces for material to be filled in using a separate deposition device (often a secondary vacuum mechanism). However, extensive analysis has shown contamination of one section with un-sintered material from another using the outlined methods is a persistent problem [19–22].

Other approaches for multi-material laser sintering include LENS/

* Corresponding author.
E-mail addresses: jdw2199@columbia.edu (J. Whitehead), hod.lipson@columbia.edu (H. Lipson).

https://doi.org/10.1016/j.addma.2020.101440
Received 3 December 2019; Received in revised form 26 June 2020; Accepted 6 July 2020
Available online 08 July 2020

DED processes which jet multiple powders into the focal point of a laser beam [23]. The LENS process has many advantages including the ability to add material to existing parts and conform to existing complex geometries, but is generally wasteful in powder usage since the powders cannot be easily separated or retrieved after the spraying. Additional approaches are currently in development that would allow for multi-material printing but are not yet commercially available and would require users to purchase special powders to act specifically as support structures.

1.3. Inverted laser sintering (ILS)

In this paper, we present a LS process design which sinters material particles together by directing the laser vertically upwards into a thin layer of powder through a borosilicate glass pane underneath the print bed. We call this process Inverted Laser Sintering (ILS).

The first step of ILS involves coating the upper surface of the glass with a release agent and depositing a controlled quantity of material on top of this glass, distributing the powder evenly using vibration to form a monolayer. Excess material can be removed using a vacuum device, as the release agent captures a single layer of powder. Note that the release agent is not strictly necessary, and powder could also be distributed freely directly onto the glass plate, however we found that use of a release agent delivered consistent results.

Next, a substrate is pressed on top of the unfused powder monolayer, and a blue laser is used to selectively fuse the particulate material onto this substrate. Finally, the substrate is lifted, and the material on the powder glass plate is replenished. This process can be repeated, with the new material layer fusing to the previous material layer, until the print is completed (Fig. 1). A force can be applied to help increase adhesion between the sintered material and the print platform or previous layers, and increase the density of the resulting part.

Using multiple glass plates in parallel, it is possible to use multiple materials, thereby enabling the manufacture of graded and multi-material parts [24]. Multi-material fabrication is accomplished by transporting the substrate between separate glass panes containing different materials, preventing the particle mixing which would be caused by multiple materials in a single, traditional LS process print bed. Multiple glass beds with identical material could also be used in parallel to accelerate the processing, so that one bed is being prepared while the other is being used.

Transporting the part between multiple print beds also allows for an integrated cleaning mechanism which removes any loose powder, in order to prevent cross-contamination. This method of printing would also reduce the amount of material needed to generate a part by eliminating the need for surrounding passive support material bed, thus reducing the amount of material needed to be exposed to a heated environment to generate the print.

Furthermore, the ability to raise and lower the printing platform allows for active compression of the un-sintered material between this platform and the glass, increasing part strength by decreasing porosity.

1.4. Caveats

While the previously mentioned benefits of our design address several crucial problems that challenge traditional LS processes, a full ILS system would likely have some downsides when compared to a standard LS system as well. Due to the use of multiple glass panes, as well as a moveable print substrate, powder deposition system and other mechanisms necessary for printing in this way, the ILS system would be more complex than a conventional LS printer, resulting in more potential points of failure. Also, since prints generated using our design no longer have passive material to act as support, parts generated by our printer could potentially be constricted in terms of geometric complexity.

Additionally, exposure of the material to the laser through the glass can cause mild adhesion between the pane and the print layer if the release agent is not utilized. This adhesion could potentially cause tearing when the substrate is raised if the printer is improperly calibrated, or contamination through the glass bed itself. The movement of the substrate/print would also slow down the generation speed of the print, both during raising and lowering and movement between different glass plates.

Furthermore, due to our use of a blue laser, a substrate that effectively absorbs blue light or a thermally activated adhesive is key to ensure adhesion of the initial print layers to the platform.

2. Materials and methods

2.1. Testing setup

To test this concept, we developed a system for fusing two thermoplastic polymers into a single layer. For our laser setup, we used a 2.8 W blue laser (445 nm, J Tech Photonics), which was tuned down to 1.3 W at 1.25 amps to increase the system's longevity and reduce heat generation. The laser was directed towards the intended sintering

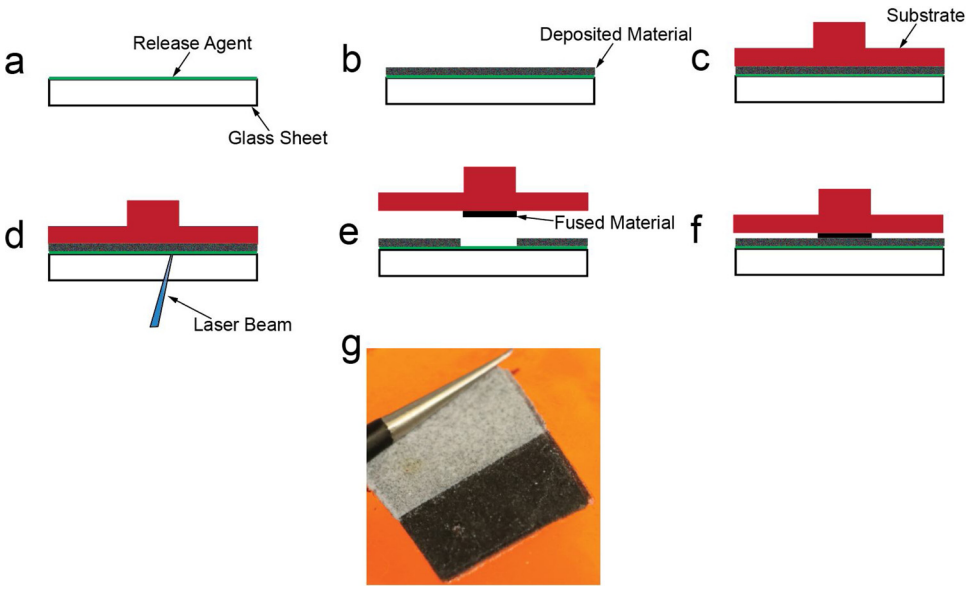

Fig. 1. Overview of the inverted sintering process (a) A release agent (green) is distributed over the upper surface of the glass (b) Unfused material (gray) is distributed over the release agent and the excess is removed (c) The build plate onto which the substrate is attached (red) is placed on the material surface (d) The laser (blue) is run in a pre-programmed pattern (e) The build plate with the fused material is lifted and the unfused material can be replenished or moved to a different glass sheet (f) The process is repeated with a new layer of material and release agent (g) Multi-material sample generated with this process.

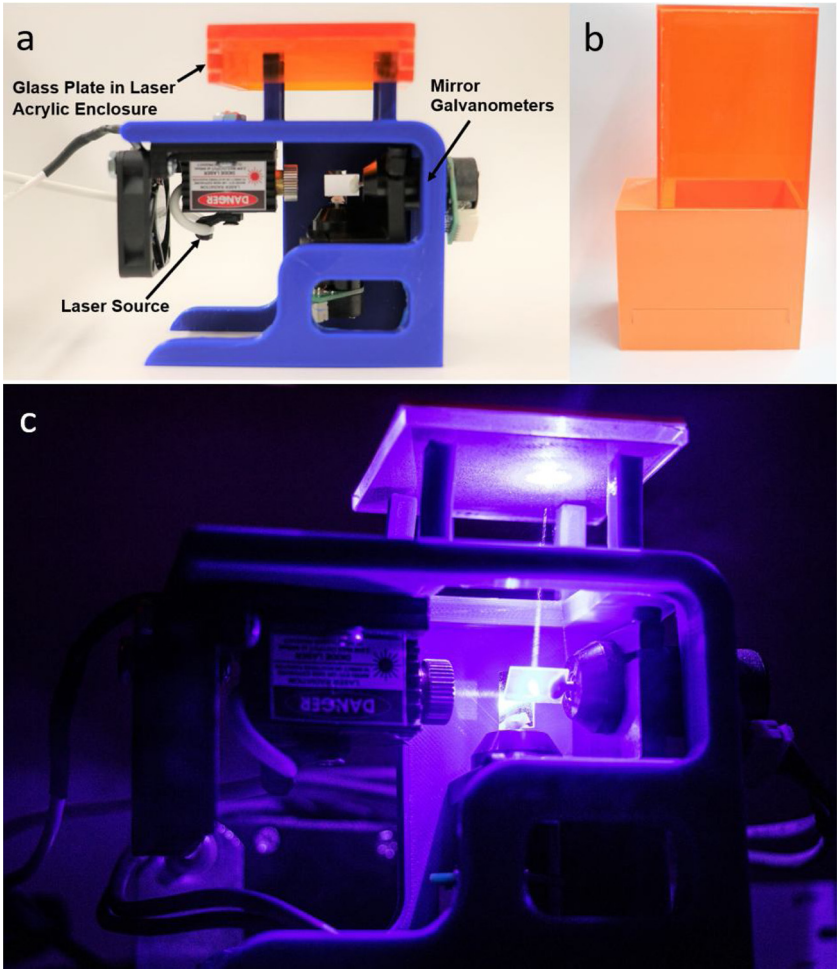

Fig. 2. (a) Inverted laser setup attached to a 3D printed mount (b) Laser opaque containment unit (c) Laser in its operating state without the containment unit in place showing the beam directed up into a glass piece.

location by a set of mirror galvanometers (Seeed Studios) controlled by an Arduino Uno. A standard CO_2 laser was not selected as it would interact with our chosen clear glass, whereas a blue laser transmits directly through into the material.

Our system (Fig. 2) was constructed with the mirrors directing the beam upwards. To prevent adhesion between the laser affected material and the glass, an optically clear release agent was reapplied to the glass between each sintering cycle. The release agent we chose (Water Soluble Mold Release Agent, SLIDE) was selected because of its maximum operating temperature (232 ˚C), its optical clarity, and the fact that it is water soluble which would allow for its potential removal from any unsintered material.

To mitigate the chance of damage to the testing surroundings, an orange inverted powder bed was constructed of laser protective acrylic (Laser Shielding, J Tech Photonics), and all single layer experiments were conducted within this area. The acrylic used is opaque to lasers in the 250 nm–520 nm spectrum, and would therefore be damaged by the laser instead of allowing the beam to directly transmit through. For multi-layer experiments, a secondary containment unit was fabricated out of 3D printed PLA and orange acrylic to house the entire laser system. Additionally, an alignment mechanism was 3D printed to replace the acylic powder bed, to ensure repeatable alignment and placement of the glass and substrate from layer to layer.

2.2. Multi-material selection

Two different powders were needed to allow us to demonstrate the multi-material printing capabilities of our printer concept. The first one selected was Nylon 12, also known as PA12 (dark gray, Sintratec Ltd). This material was chosen for three reasons.

First, PA12 is a commonly used and widely available LS material, which makes the powder easier to find commercially in smaller quantities (~2 L containers) [25]. Second, PA12 is a thermoplastic material, implying that this powder has a relatively low sintering temperature (~176˚C) when compared to glass or metal powders [26]. This low melt temperature was especially important for our testing, as we do not utilize a heated print environment; therefore, we do not, at this point, benefit from an initial temperature baseline increase. Third, PA12 has been used in existing commercial desktop LS printers which incorporate blue lasers in a traditional downwards facing configuration [27].

White TPU (Sinterit) was the second material selected. This selection was due to the color difference, which makes the distinction between the two materials in a printed part visually apparent, as well as TPU's melting temperature (~160˚C), which is comparable to the Nylon's. In this work, this comparable melting temperature is necessary as we kept the laser's power fixed during all testing. However, changing the laser's operating power in future experiments would allow for the use of a wider array of materials.

2.3. Refraction compensation

The use of a glass slide introduces optical refraction into the LS process, changing the location and overall shape of the print layer being generated. In order to test the effect of the laser on our chosen materials

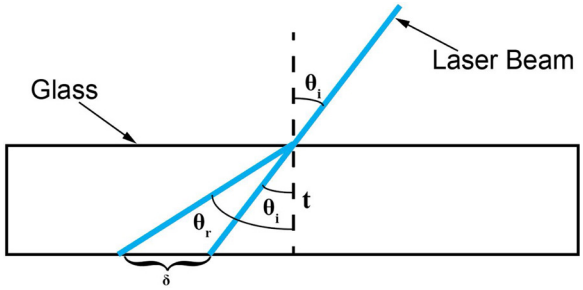

Fig. 3. Diagram of laser refraction.

through a clear medium, we purchased borosilicate glass, which was selected due to the glass' relatively low coefficient of thermal expansion [28]. A low coefficient was necessary to ensure the glass would not fail during the repeated heating and cooling cycles inherent in our process [29]. The position change of the beam can be calculated by first determining the angle of refraction from Snell's law (Eq. 1) [30]:

$$\theta_r = \arcsin\left(\frac{n_i * \sin(\theta_i)}{n_r}\right) \quad (1)$$

Where n_i is the refractive index of the incident medium (air, ~1), n_r is the refractive index of the glass (~1.47), θ_i is the incident angle of the beam and θ_r is the refraction angle (Fig. 3). Taking both angles we calculated the distance from the point where the beam entered the glass to the point of sintering projected onto the material with and without the refraction (respectively) using (Eqs. 2 & 3):

$$\delta_i = t * \tan(\theta_i) \quad (2)$$

$$\delta_r = t * \tan(\theta_r) \quad (3)$$

The difference between the two distances is the beam offset cause by the glass projected onto the material plane (Eq. 4):

$$\delta = t * (\tan(\theta_r) - \tan(\theta_i)) \quad (4)$$

Where δ is the offset between the expected sintering point (without beam refraction) and the actual sintering point, and *t* is the thickness of the glass. For our calculations we assume the laser directly transmits from the bottom side of the glass into the material without any additional intermediary refractive index. The calculated offset informed our decision to maximize the distance from the laser to the glass, to reduce the distance between the laser and any sintering point, thus decreasing the incident angle. Additionally, we limited the thickness of the glass (~3.175 mm) and the size of our maximum sintering area (50.8 mm by 50.8 mm) to further decrease any print deformation. However, as our focus was primarily to prove the concept, outside of the construction of our physical setup, we largely ignored refraction effects during testing.

2.4. Testing

2.4.1. Sintering parameters

To increase adhesion of the sintered material to the passive print platform, we incorporated a pre-made substrate fabricated from laser opaque orange acrylic. As our substrate is also made of a thermoplastic, the powders we are using can effectively bond to its surface. The actylic substrate could also be fabricated from a different thermoplastic (i.e. ABS) which could be easily dissolved, such as through submersion in acetone.

Multi-material sintering was done initially using a rectangular spiral pattern due to the shape's ability to be easily tessellated. Determination of parameters for the rectangular spiral pattern focused on the spacing between consecutive spirals and the laser propagation speed to affect print layer generation. The propagation speed was controlled by the distance between successive points of laser exposure in the spiral pattern, as well as the time delay between moving from one point to the next (Fig. 4a). In addition to the rectangular spiral, a larger print sample was generated using a single material with the laser in a concentric circle configuration. Parameters for each circular layer include the angle between successive sintering points in a given circle and the distance between circles, as well as the time delay between moving from one point to the next (Fig. 4b). These factors all directly have an effect on sintering time to completion. Settings were constant for the entire laser pattern.

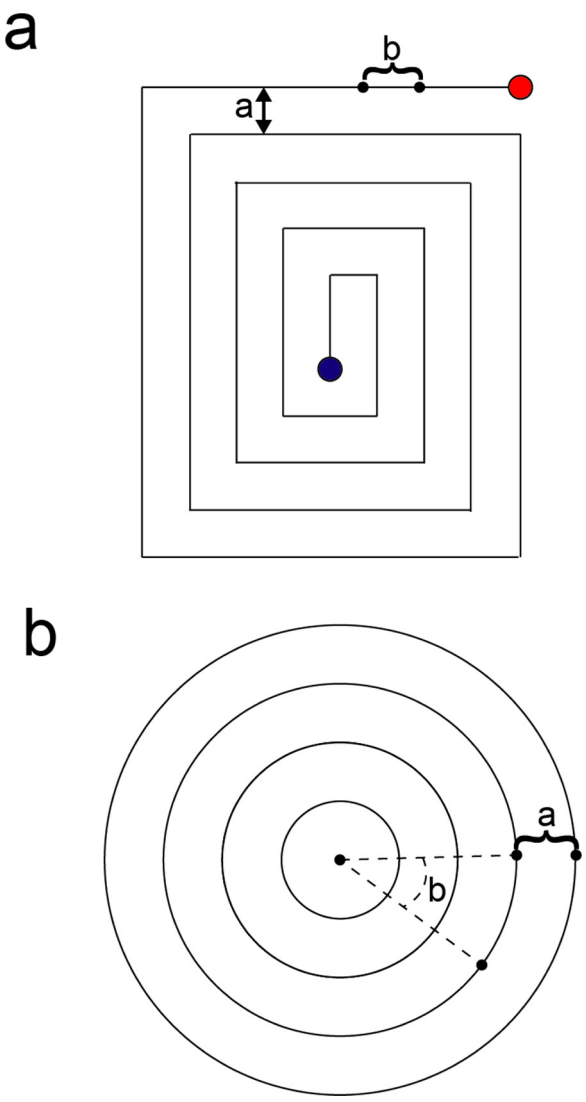

Fig. 4. (a) Rectangular spiral sintering pattern diagram, parameter a is the spacing between consecutive spirals, and parameter b is the laser propagation speed. Sintering starts at the red dot and ends at the blue. (b) Concentric circle sintering pattern diagram, parameter a is the spacing between consecutive circles, and parameter b is the angle between successive sintering points. A sintering cycle starts at the outermost circle and moves inwards.

Testing was done by adjusting the parameters, taking into account the melting temperatures of the different materials, and the color differences which affect the absorption of the laser energy. As a result, different parameters were chosen for the two different materials. Parameters were adjusted to ensure sintering of the material while reducing time to completion of the spiral pattern.

2.4.2. Print strength and laser melting depth

The use of a platform which can be raised and lowered allows for variable loading pressures during each layer's generation by using the platform to compress the material between the substrate or the previous

print layer and the glass with a controlled amounts of force. This has the potential to directly affect part density, either by changing the uniform density of the part or allowing for different densities throughout by applying different loads at different layers.

To test the effects of applied loading, we generated print samples using our ILS setup by placing ~2 g of material on the glass without the release agent, distributed across the surface both with and without the compression of a 1 kg weight (Troemner). With our pre-determined parameters, this amount of material was found to be a sufficient quantity that it, when evenly spread over the glass, was enough to prevent the laser from penetrating all the way through. The laser then sintered a rectangular spiral through the glass, generating a print layer with outer dimensions of approximately 18.27 mm by 16.16 mm. The 1 kg load was evenly distributed over the material undergoing compression, resulting in a pressure of 33.2 kPa on the powder surface. After sample generation, the excess material was manually disposed of, and the resulting print sample was removed from the glass and subsequently tested.

Tests were conducted with the TPU powder. After samples were generated, they were strained in an Instron 5569 until failure to determine ultimate force and displacement. After testing, samples were disposed of.

In addition to determining the performance of raw material undergoing different loading conditions, we generated equivalent samples from material that had been exposed to our selected release agent to measure if it had some measurable impact on the mechanical properties of a sintered powder layer. This was to determine if the excess material in a print layer could be reused without post-processing. We accomplished this by directly applying the agent to a controlled quantity of material, then allowing sufficient time (~2 days) for complete evaporation of any fluids, leaving behind solely the TPU and any residue that might remain as a coating on the material. The affected powder was then collected and tested in the same manner as the compressed, unaffected material using the same laser parameters. The resulting sample data was compared to that of the unaffected material.

2.4.3. Inverted print generation

To validate the ILS printer design, a multi-layer print was generated out of the TPU and Nylon powders with the laser in an upwards directed configuration. This was done by first coating the upper surface of the borosilicate glass with the release agent. This release agent both prevents the material from adhering to the glass during sintering, but also its liquid state, in combination with its viscosity, efficiently captures a single uniform layer of powder for sintering across the glass surface. After the agent is applied, TPU powder was manually distributed over the surface of the glass, and the layer was visually inspected to ensure that the entire surface was coated. As this manual material deposition process results in more material distributed on the glass than can be captured by the release agent or penetrated through by the laser, excess material is removed using a vacuum system which leaves only the material layer captured by the release agent. The thickness of this powdered material layer, therefore, depends in part on the quantity of the release agent layer distributed on the glass. Due to the fact that experiments were conducted manually, there is naturally going to be some slight variance in layer thickness. A mechanical test setup could correct this using a precise, mechanical, timed sprayer with a feedback mechanism, or a roller mechanism which could ensure a uniform layer height, as is the case in traditional SLS printers.

Selective material or release agent deposition can potentially be incorporated to allow for multiple materials on the same glass slide or to reduce material exposure to the release agent. The material-coated glass is then placed above the mirror galvanometer array, a substrate is lowered on top, and a 33.2 kPa load was applied to increase adhesion. The laser is directed in a square spiral pattern or concentric circles to sinter the new layer to the previous layer(s).

Once the TPU rectangle has been completed, the load and substrate with the fused material are removed, and the glass is replaced with an identical glass piece coated with a single print layer of Nylon, also captured using the release agent. The substrate and load are placed on this new glass and the laser is run again to fuse a Nylon spiral adjacent to the TPU spiral, in the same layer. Between each layer, all unfused material was removed from the glass using a rubber scraper, which could be incorporated into a complete printer setup, and the glass was recoated with new material and release agent. This generates a multi-material sintered sample with multiple materials in the same layer. The process is similar for a single material print, the only difference being the lack of material change.

3. Results

3.1. Sintering parameters

To determine the heating profiles of the selected materials during the spiral generations, we directly monitored the heated material using a thermal camera (C2 Thermal Imaging Camera, FLIR) with imaging in the 7.5–14 μm spectral range and ~0.94 emission coefficient. This was accomplished by temporarily placing the laser in a downward configuration and distributing material evenly in a reservoir in the path of then laser without anything between the powder and beam. This downward configuration was necessary as we wanted to directly monitor heating at the point of interaction between the laser and the powder, which would have been challenging with the glass acting as insulation.

The maximum temperatures recorded during the sintering process for the Nylon and the TPU were both found to be ~180°C at the center of the spiral, increasing from an ambient temperature of ~30°C (Fig. 5). We note that the maximum temperature in the sintering pattern increases as the laser reaches the center of the spiral. This is likely due to the decreased time between when the laser reaches a point near where the beam previously sintered material, allowing for less cooling time. Additionally, due to the camera's limited maximum temperature detection capabilities (180°C), higher temperatures were likely reached towards the spiral's center and not recorded, as evidenced by plateaus in the graphs.

The use of the release agent allows for a substantial range of possible sintering parameters. This is due to the fact that the incorporation of this spray prevents any material adhesion to the glass during sintering, rendering exposure time of the laser to the material trivial. However, in order to prevent over-sintering, we experimentally determined parameters that would effectively fuse the material powders, both in layer and layer-to-layer while also minimizing spiral time to completion (Table 1).

3.2. Print strength and laser melting depth

As the laser did not penetrate all the way through the material deposited onto the glass, we were able to determine the maximum melting depth of the laser is ~0.3 mm for the TPU and ~0.15 mm for the Nylon (with no loading) by directly measuring maximum sample thickness with our selected parameters. The melting depth of the laser was determined to be approximately the same (~0.3 mm) for the loaded TPU. Different processing parameters would affect these values.

After the TPU samples were generated and destructively tested, the resulting force-displacement data was averaged, filtered and used to determine the average ultimate force and the corresponding displacement (Table 2, Fig. 6). Plotting was done using a moving data filer with three samples tested for each loading or spray combination condition. After the ultimate force was reached, tearing before a complete failure resulted in a peak force decrease observed on the graph, but not an immediate drop to zero. Compressing the samples lead to a clear (> 3x) peak force increase. However, the true strength variation caused by compression will likely change as a result of the sintering parameters

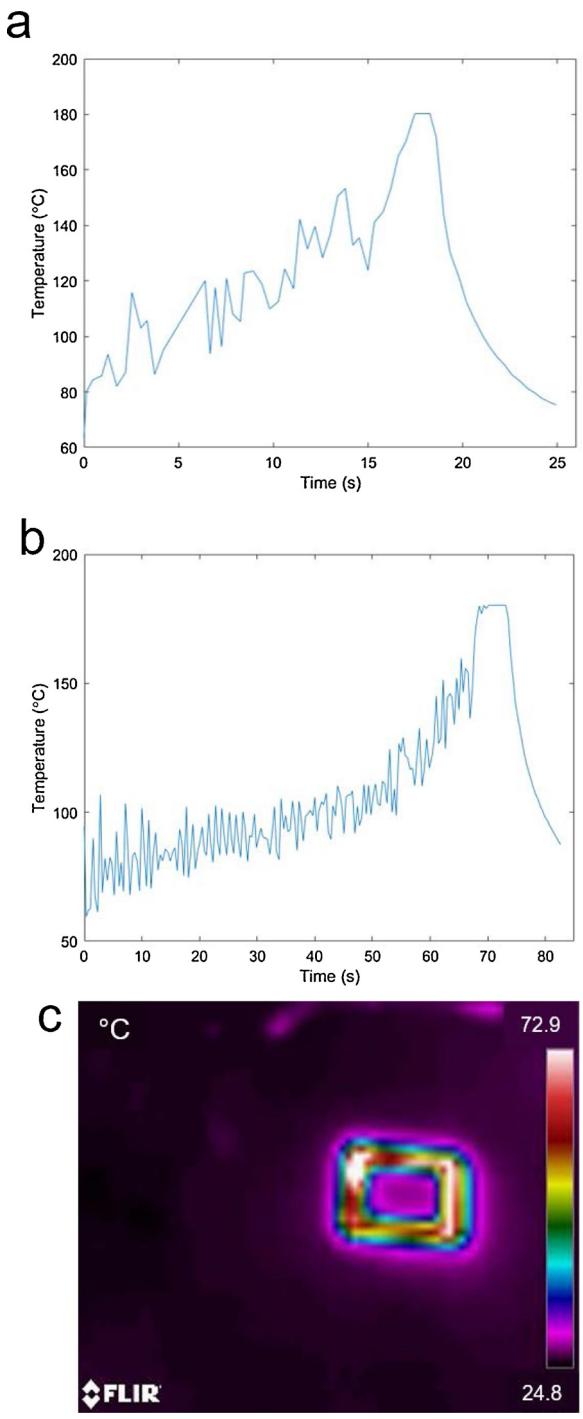

Fig. 5. Maximum temperatures recorded during the sintering spiral pattern (a) Nylon sintering (b) TPU sintering (c) Picture showing a sample heating profile during sintering.

Table 1
Sintering parameters used for testing in the ILS system.

Material	Time Delay (ms)	Exposure Distance (b)	Spiral Distance (a)
Nylon 12	0.035	4	10
TPU	0.035	20	10

used. Including a heated environment and a laser system with a higher power output would have a direct impact on the strength and porosity variation in the printed sample caused by compression. This change due

Table 2
Changes in Mechanical and Physical Properties Caused by an Applied Load on the Material During Sintering.

Loading Condition	Max Force (N)	Displacement at Max Force (mm)	Average Mass (g)
No Loading	0.64	2.97	0.051
33.2 kPa	2.09	2.28	0.042

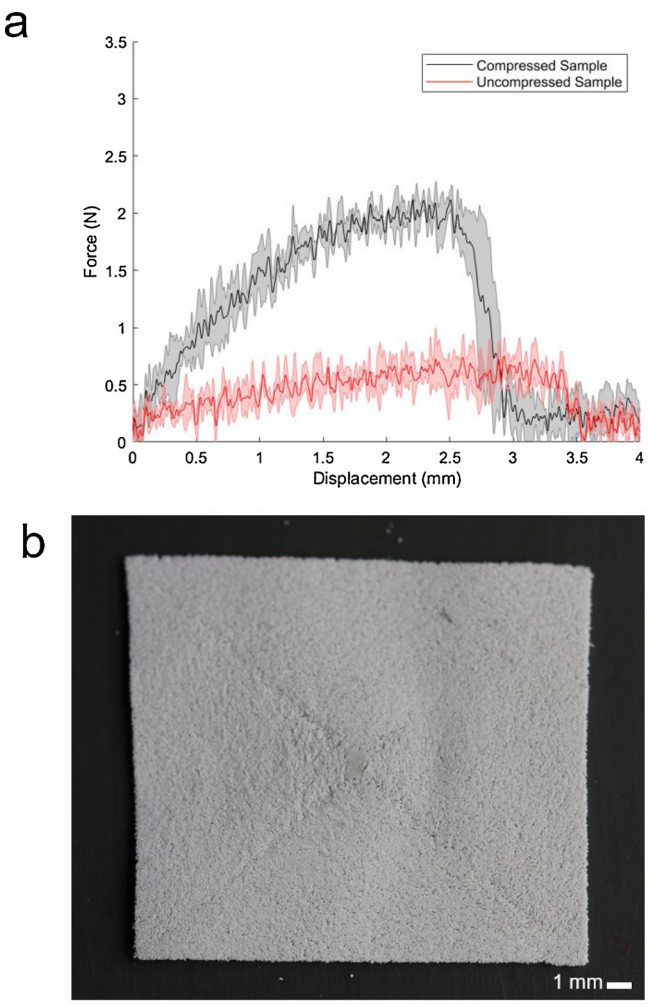

Fig. 6. Force displacement testing for loaded and unloaded samples (a) Force-displacement curves for loaded and unloaded samples, the shaded regions represent the standard deviation (b) Upper surface of unloaded test sample.

to different loading conditions would allow for a designed point of failure in the print that is artificially weaker.

Samples which underwent loading had a noticeably lower average mass. Additionally, closer inspection of the print surface showed that compressed samples had a less porous surface in contact with the glass. This implies to us that the laser overall penetrates approximately the same distance in both samples (as evidenced by maximum sample thicknesses), but creates a much steeper density gradient in the compressed sample due to the beam's inability to easily affect material above the more homogeneous surface in contact with the glass. An analysis of sample cross sections appears to confirm this hypothesis (Fig. 7). Sintering a thinner deposited layer of un-sintered material, with a limited thickness of ~50 μm would likely create a more vertically homogenous, stronger compressed sample, with a weight higher than the uncompressed equivalent.

Print samples that were generated from release affected material

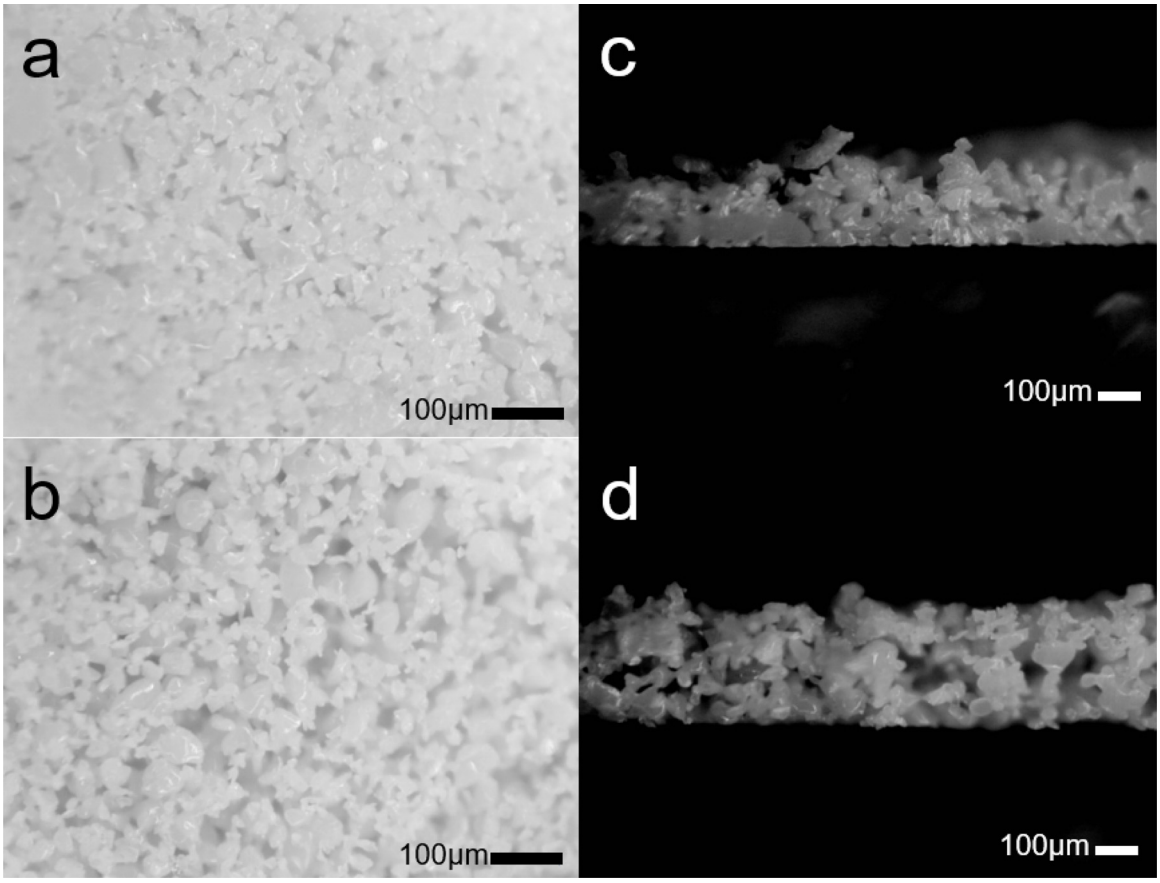

Fig. 7. Close-Up images of the laser affected material (a) Loaded sample side in contact with glass (b) Unloaded sample side in contact with glass (c) Cross sectional view of the loaded sample (d) Cross sectional view of the unloaded sample.

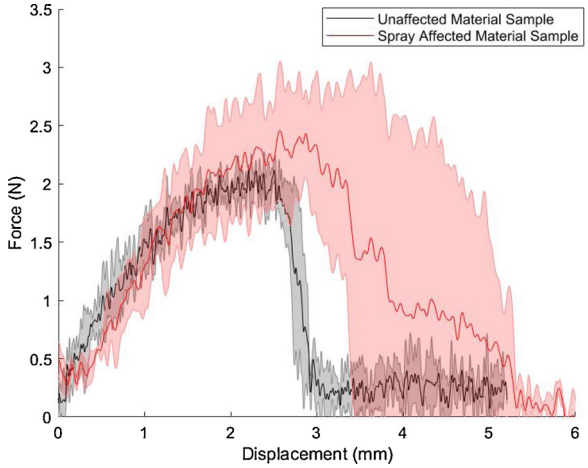

Fig. 8. Force displacement testing for agent affected and unaffected samples.

underwent the same destructive testing and data filtering procedure as the compressed/uncompressed samples, also with three test samples (Fig. 8). Both the affected an unaffected material have similar force-displacement curves, with overlapping error bounds. This implies that the introduction of our release agent has a mild effect on the strength of the part in any given layer. This effect appears to, however, introduce a greater amount of unpredictability into the sintered material's behavior. This unpredictability may change with further trials or greater exposure to the laser, which could further burn off any transients. Additionally, due to the sintering temperature difference, metal powders might suffer even less from exposure to the release agent. Any residue remaining on the final printed part can be washed off as the release agent is water soluble if desired. The application of this release agent could potentially cause reduced layer adhesion if it is not removed between layers.

3.3. Inverted print generation

We generated a multi-layer inverted print pattern which was 11 layers thick and had an overall height of 0.78 mm (Fig. 9). Usage of the release agent to evenly distribute material resulted in a far more uniform height from layer to layer, resulting in a part with a more homogeneous thickness. The average layer thickness was found to be ~71 μm, calculated by dividing the overall height of the sample by the number of layers. Utilizing a conventional material spreading method (e.g. rollers) could potentially increase print resolution and reduce layer unevenness and non-uniformity. This ILS print generation was done using the parameters outlined in Table 1. As expected, the print outline was slightly distorted due to the refraction caused by the glass. It can be seen that particle cross-contamination occurred in the print due to imperfect removal of un-sintered material from the previous material rectangle generation. We believe that incorporating a precision cleaning mechanism to remove excess material would be an effective way to eliminate accidental impurities. Once implemented, cross contamination levels would need to be quantified. A more in depth study of the accuracy of the process will be included in future work when an automated testing setup has been constructed.

In addition to our multi-material print, we generated a multi-layer, single material print using the TPU powder with the circular sintering pattern (Fig. 10). This print consisted of 50 layers, with an average outer diameter of ~20 mm, and inner diameter of ~4 mm. This print

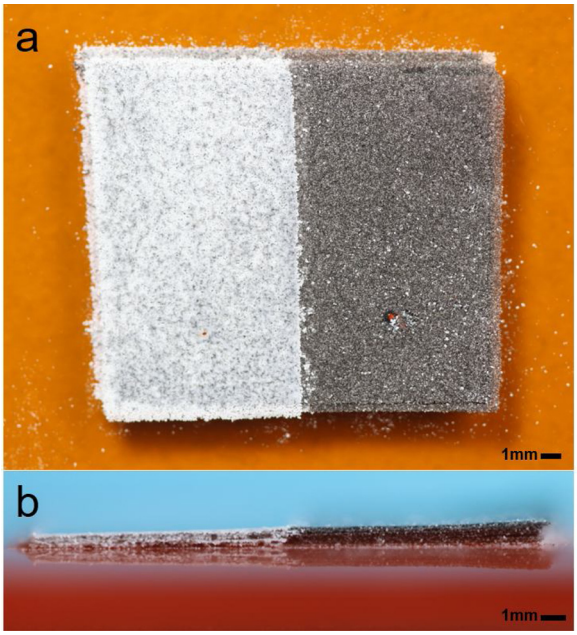

Fig. 9. Inverted multi-material sintering pattern on an acrylic substrate (a) Top view (b) Profile view.

has an overall height of 2.18 mm. This results in an average layer height of 43.6 μm. This sample was generated using a time delay of 5 ms, a successive circle difference (a) of 20 and an angular distance (b) of 1 degree. As the input shape parameters should have resulted in a perfect circle, the minor part distortion due to the refraction from the glass is clearly visible. We were able to remove this part from the substrate using a razor to observe the point of contact between the print and the platform. This print was again generated with a load applied to the substrate.

4. Discussion

4.1. Layer generation

The relatively minor temperatures reached during majority of the laser cycle implies that the print samples generated were under sintered, reducing the ultimate amount of stress that our test prints could sustain. The use of a more uniform processing method, such as rastering, would likely result in a more uniform sample and heating profile. Additionally, changing the propagation parameters of the laser in the spiral pattern so the beam speed increases towards the center of the spiral would even out the laser exposure time to the material, which could result in a more homogenous print layer. Knowing the maximum laser melting depth for a given set of parameters is key to determining optimal print layer thickness. Calibration of a printer to have a possible layer thickness greater than the maximum possible melting depth would make layer adhesion impossible.

Though the glass was recoated between each layer, we have shown that material directly affected by the release agent can be reused to generate print layers with mechanical properties similar to unaffected material. This allows for un-sintered material to potentially be collected and reused. As the used release agent is water soluble, this would also present a possible method to remove it from the unused material. Additionally, in between each layer, any residue that remains on the glass due to the release agent or the sintering process after excess material is removed can be taken care of by directly incorporating a glass cleaning apparatus into the printer design.

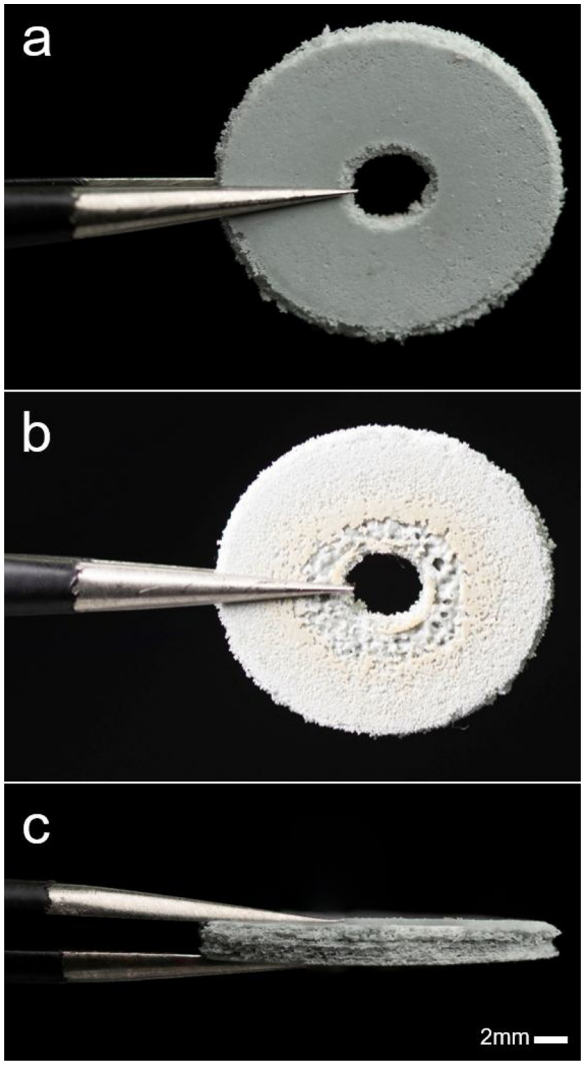

Fig. 10. Inverted 50 layer sintering sample (a) Top view (b) Bottom view (c) Profile view.

4.2. Inverted print generation

The layer thickness of our inverted print (71 μm) is well within the standard range of layer thicknesses for LS printers of (20 − 150 μm) [31]. The use of a direct compression mechanism ensures adhesion of material to the previous layer(s) or substrate regardless of powder thickness change cause by heating of the material. Furthermore, the use of our release agent to “capture” a single powder layer allows for the repeatable retention of a given layer thickness of material as a function of the quantity of release agent and powder distributed on the glass. Compression of material layers can potentially be used to change their thickness, directly affecting layer adhesion.

The individual layer height (43.6 μm) for our 50 layer print again falls within the standard range for SLS prints. The drastic difference between the layer height in the multi-material print and the 50 layer print can potentially be contributed to a variety of factors. As the thickness of a print layer is directly connected to the amount of release agent used, the manual nature of the two different print generations can lead to greater variation in the amount of agent applied, leading to greater variation in print layer. The different settings use in the generation of the different samples can also potentially be a contributing factor. We believe that a more precise printer setup with a consistent processing pattern will have greater control over the layer height from print to print.

Inspection of the lower layers of the 50 layer print once removed from the substrate allows us to see that some of the orange from the substrate remains on the print and the bottom layers are not as uniform as the upper layers. This implies the need for the first few layers printed to be sacrificial layers which can be removed from the print after it is removed from the substrate.

4.3. Future work

Now that we have successfully demonstrated our ability to sintering material through glass to a thermoplastic substrate, our next step will be to fully construct a printer setup with an ILS. This setup will include automatic powder deposition, as well as vibration-enabled powder leveling. Future design iterations could incorporate a roller powder deposition that does not require the use of a release agent for holding a single material layer. This would negate the need for material post processing to remove the residue from the unsintered material. We believe a more precise machine will generate stronger parts with greater resolution. Part generation will need to be automated to reduce production time and to increase layer uniformity. Additionally, direct compression of the parts during printing has the potential to deform the object being generated, which a full printer setup would allow us to measure and observe. This deformation would be a function of material, layer cross sectional area.

We also will experiment with replacing the mirror galvanometer and stationary laser with a moving blue laser source or a lens to compensate for refraction to severely reduce layer border irregularity in order to increase print quality and enable generation of more complex designs. Laser parameters will be further optimized, incorporating variable speed to ensure that no one section of the part receives greatly more laser exposure than any other to prevent the creation of any weak spots are unintentionally fabricated due to excessive or insufficient heating. Further work will also include characterizing more uniform parts printed in this way. Additionally, we will be expanding testing to incorporate a wider range of materials including metal alloys such as stainless steel to allow for stronger printed parts. For the sintering of higher melting point materials (e.g. metals), stronger transparent plates (such as quartz and sapphire glass) will need to be used, as well as release agents that are able to sustain the increased temperatures.

5. Conclusion

In this paper we have outlined a novel laser sintering process that utilizes an inverted laser to sinter two thermoplastic powders through a glass plate onto a moveable print platform. This printing process allows for multi-material laser sintering 3D printing with direct control of the print's mechanical properties.

Reduced material usage is enabled because our design does not have passive, un-sintered material surrounding the part at each layer, which is both wasteful and obscures the part during fabrication, making part inspection before the process is completed nearly impossible.

Additive manufacturing of multiple materials with the proposed design has the potential to expand laser sintering into a wider variety of industries by allowing for fabrication of complex multi-material parts without any assembly.

Future work will cover the use of conductive and metallic powders, which would allow us to directly generate parts with a wider range of mechanical, electrical and chemical properties than is possible with conventional LS systems today.

CRediT authorship contribution statement

John Whitehead: Writing - original draft, Conceptualization, Visualization, Data curation. **Hod Lipson:** Writing - review & editing, Conceptualization.

Declaration of Competing Interest

No competing financial interests exist.

Acknowledgements

The authors acknowledge Jonathan Blutinger for assistance in setting up the laser.

Appendix A. Supplementary data

Supplementary material related to this article can be found, in the online version, at doi:https://doi.org/10.1016/j.addma.2020.101440.

References

[1] T.T. Wohlers, I. Campbell, O. Diegel, J. Kowen, Wohlers Report 2018: 3D Printing and Additive Manufacturing State of the Industry: Annual Worldwide Progress Report, (2020) n.d..
[2] The State of 3D Printing Edition, The State of 3D Printing Edition, (2018) (Accessed April 23, 2019), https://www.sculpteo.com/media/ebook/State_of_3DP_2018.pdf.
[3] I. Anderson, Mechanical properties of specimens 3D printed with virgin and recycled polylactic acid, 3D Print. Addit. Manuf. 4 (2017) 110–115, https://doi.org/10.1089/3dp.2016.0054.
[4] K.R. Bakshi, A.V. Mulay, A Review on Selective Laser Sintering: A Rapid Prototyping Technology, (2020) www.iosrjournals.org.
[5] S. Kumar, Selective laser sintering: a qualitative and objective approach, JOM 55 (2003) 43–47, https://doi.org/10.1007/s11837-003-0175-y.
[6] M. Agarwala, D. Bourell, J. Beaman, H. Marcus, J. Barlow, Direct selective laser sintering of metals, Rapid Prototyp. J. 1 (1995) 26–36, https://doi.org/10.1108/13552549510078113.
[7] J.P. Kruth, X. Wang, T. Laoui, L. Froyen, Lasers and materials in selective laser sintering, Assem. Autom. 23 (2003) 357–371, https://doi.org/10.1108/01445150310698652.
[8] S. Jasveer, X. Jianbin, Comparison of different types of 3D printing technologies, Int. J. Sci. Res. Publ. 8 (2018), https://doi.org/10.29322/IJSRP.8.4.2018.p7602.
[9] J.M. Williams, A. Adewunmi, R.M. Schek, C.L. Flanagan, P.H. Krebsbach, S.E. Feinberg, S.J. Hollister, S. Das, Bone tissue engineering using polycaprolactone scaffolds fabricated via selective laser sintering, Biomaterials 26 (2005) 4817–4827, https://doi.org/10.1016/J.BIOMATERIALS.2004.11.057.
[10] J.V. Williams, P.J. Revington, Novel use of an aerospace selective laser sintering machine for rapid prototyping of an orbital blowout fracture, Int. J. Oral Maxillofac. Surg. 39 (2010) 182–184, https://doi.org/10.1016/J.IJOM.2009.12.002.
[11] T. Gornet, K. Davis, Characterization of Selective Laser Sintering Materials to Determine Process Stability, Sffsymposium.Engr.Utexas.Edu. T.S.-S.F., undefined, (n.d.)http://sffsymposium.engr.utexas.edu/Manuscripts/2002/2002-62-Gornet.pdf (Accessed April 23, 2019) (2002).
[12] K. Dotchev, W. Yusoff, Recycling of polyamide 12 based powders in the laser sintering process, Rapid Prototyp. J. 15 (2009) 192–203, https://doi.org/10.1108/13552540910960299.
[13] A. Drizo, J. Pegna, Environmental impacts of rapid prototyping: an overview of research to date, Rapid Prototyp. J. 12 (2006) 64–71, https://doi.org/10.1108/13552540610652393.
[14] S. Singh, A. Sachdeva, V.S. Sharma, Investigation of dimensional accuracy/mechanical properties of part produced by selective laser sintering, Int. J. Appl. Sci. Eng. 10 (2012) 59–68, https://doi.org/10.6703/IJASE.2012.10(1).59.
[15] G. Guan, M. Hirsch, W.P. Syam, R.K. Leach, Z. Huang, A.T. Clare, Loose powder detection and surface characterization in selective laser sintering via optical coherence tomography, Proc. Math. Phys. Eng. Sci. 472 (2016), https://doi.org/10.1098/rspa.2016.0201 20160201.
[16] C.L. Liew, K.F. Leong, C.K. Chua, Z. Du, Dual material rapid prototyping techniques for the development of biomedical devices. Part 1: space creation, Int. J. Adv. Manuf. Technol. 18 (2001) 717–723, https://doi.org/10.1007/s001700170014.
[17] H.-C. Kim, J.-W. Choi, E. MacDonald, R. Wicker, Slice overlap-detection algorithm for process planning in multiple-material stereolithography, Int. J. Adv. Manuf. Technol. 46 (2010) 1161–1170, https://doi.org/10.1007/s00170-009-2181-x.
[18] J. Santosa, D. Jing, S. Das, Experimental and Numerical Study on the Flow of Fine Powders From Small-Scale Hoppers Applied to LS Multi-Material Deposition–Part I, Sffsymposium.Engr.Utexas.Edu. (n.d.). http://sffsymposium.engr.utexas.edu/Manuscripts/2002/2002-70-Santos.pdf (Accessed April 26, 2019) (2020).
[19] K. Lappo, B. Jackson, D. Wood, Discrete multiple material selective laser sintering (M2LS): experimental study of part processing, Solid Free. Fabr. Symp. Univ. Texas, Austin, TX 6 (2003) 109–119 (Accessed June 24, 2019), https://www.researchgate.net/publication/270158698_Discrete_multiple_material_selective_laser_sintering_M2LS_Experimental_study_of_part_processing.
[20] Y. Chivel, New approach to multi-material processing in selective laser melting, Phys. Procedia 83 (2016) 891–898, https://doi.org/10.1016/j.phpro.2016.08.093.
[21] M. Vaezi, S. Chianrabutra, B. Mellor, S. Yang, Multiple material additive manufacturing – part 1: a review, Virtual Phys. Prototyp. 8 (2013) 19–50, https://doi.org/10.1080/17452759.2013.778175.

[22] C. Wei, L. Li, X. Zhang, Y.H. Chueh, 3D printing of multiple metallic materials via modified selective laser melting, CIRP Ann. 67 (2018) 245–248, https://doi.org/10.1016/j.cirp.2018.04.096.
[23] M.L. Griffith, D.L. Keicher, J.A. Romero, C.L. Atwood, L.D. Harwell, D.L. Greene, J.E. Smugeresky, Laser engineered net shaping (LENS) for the fabrication of metallic components, 12. Annu. Meet. Jt. Work. Gr. (JOWOG-31), Livermore, CA (United States), 13-16 May 1996 (1996) (Accessed July 17, 2019), https://digital.library.unt.edu/ark:/67531/metadc667090/.
[24] S. Kaijima, Y.Y. Tan, T.L. Lee, Functionally Graded Architectural Detailing Using Multi-Material Additive Manufacturing, (2017) (Accessed July 3, 2019), http://papers.cumincad.org/data/works/att/caadria2017_142.pdf.
[25] N. Clark, F. Lacan, A. Porch, Microwave measurements of nylon-12 powder ageing for additive manufacturing, Solid Free. Fabr. 2017 Proc. 28th Annu. Int., Solid Freeform Fabrication Symposium (2017) (Accessed April 23, 2019), http://sffsymposium.engr.utexas.edu/sites/default/files/2017/Manuscripts/MicrowaveMeasurementsofNylon12PowderAgeingf.pdf.
[26] M. Vasquez, B. Haworth, N. Hopkinson, Optimum sintering region for laser sintered nylon- 12, Proc. Inst. Mech. Eng. Part B J. Eng. Manuf. 225 (2011) 2240–2248, https://doi.org/10.1177/0954405411414994.
[27] I.P.F. Richards, T.M.N. Garabet, I.S. Bitar, F.M. Salmon, Optimising thermoplastic polyurethane for desktop laser sintering, Solid Free. Fabr. 2017 Proc. 28th Annu. Int., Solid Freeform Fabrication Symposium (2017) (Accessed April 23, 2019), http://sffsymposium.engr.utexas.edu/sites/default/files/2017/Manuscripts/OptimisingThermoplasticPolyurethaneforDesktop.pdf.
[28] R. Roy, D.K. Agrawal, H.A. McKinstry, Very low thermal expansion coefficient materials, Annu. Rev. Mater. Sci. 19 (1989) 59–81, https://doi.org/10.1146/annurev.ms.19.080189.000423.
[29] C.M. Cheng, Resistance to thermal shock, J. Am. Rocket Soc. 21 (1951) 147–153, https://doi.org/10.2514/8.4392.
[30] A Dictionary of Earth Sciences, Oxford University Press, 2008, https://doi.org/10.1093/acref/9780199211944.001.0001.
[31] B. Bhushan, M. Caspers, An overview of additive manufacturing (3D printing) for microfabrication, Microsyst. Technol. 23 (2017) 1117–1124, https://doi.org/10.1007/s00542-017-3342-8.